Creation of a Rigorous Human Head Model from MRI Images with Reports on SAR Caused by 2.6 GHz 5G Mobile Handset Radiation

Terapass Jariyanorawiss[1†], **Komsan Kanjanasit**[2], and **Wachira Chongburee**[1], Non-members

ABSTRACT

This research work proposes a method to rigorously model a 3D human head from the informative data in magnetic resonance imaging (MRI). The approach is based on each slice of 53 MRI resized to a 64 × 64 grayscale image to enable a practical simulation. The optimized unit cell of 5.6 × 5.6 × 5.6 mm^3 is identified as a particular type of tissue. It corresponds to the average size of an actual human brain. The material properties are assigned to various tissues of the entire structure of the human head. The computational model of this will then be used as a virtual object to study the specific absorption rate (SAR) with electromagnetic radiation (EMR) at 2.6 GHz as a 5G mid-band frequency. A commonly known finite-different time-domain (FDTD) method is used as a tool in the SAR simulation. The key results show that a handset with a power of less than 0.8 W, operating at a handset to head separation distance of 1.12 cm, will meet the FCC SAR 1g limit of 1.6 W/kg.

Keywords: Rigorous Human Head Model, Finite-Different Time-Domain, FDTD, Magnetic Resonance Imaging, MRI, Specific Absorption Rate, SAR, Electromagnetic Radiation, EMR

1. INTRODUCTION

The fifth generation (5G) of cellular technology has become a major wireless standard in daily use globally. Compared to fourth generation (4G) technology, 5G provides improved performance, including higher multi-Gbps peak data speeds, significantly lower latency, higher reliability, and massive network capacity. In order to achieve better performance than the previous generation, a new radio and network are introduced.

Three frequency spectrum bands are allocated to 5G, as follows: First is the low band of sub-1 GHz, which is suitable for urban service areas. This band needs a lower number of operational base stations to cover the designated areas. Second are the mid-bands of the sub-6 GHz (1–6 GHz). These bands can be categorized into legacy mid-bands (1–2.6 GHz) and new mid-bands (3.5–6 GHz). The coverage is less than the low band, but it allows for a higher data rate. As a result of this compromise between coverage and data rate, this band is typically used in towns and cities. Finally, 5G uses a high band of the mm-wave (24 GHz and above). Although the coverage of this band is relatively low, at around 100 meters, it has a dramatically higher data rate than the low and mid-bands. The band is therefore suitable for servicing indoor areas, such as the interior of buildings, due to lower signal attenuation and loss.

The introduction of new radio frequencies may impact on health. This research focuses on the study of the specific absorption rate (SAR) effect caused by the electromagnetic radiation (EMR) from a 5G mobile handset operating at the legacy mid-band of 2.6 GHz. The tools used in this study include an accurate human head model, a simulation technique, and a proper setup.

The human head is the critical part affected by EMR, and thus, only the head will be modeled for the SAR study. The models are created to match the physical size of an actual human head and may be either software or physical models. However, precise 3D models are not easy to create due to the various substances contained within the human head. Many models oversimplify this issue by using homogeneous fluid [1]. Some realistic models of a human head have reportedly shown unusual results [2]. Furthermore, experiments with physical models are difficult to implement in an anechoic chamber. Therefore, this research proposes a more precise model using software as a solution to investigate the SAR on the human head. Here, unit-cell optimization can be realized with an accurate size representation of a real human head and the weight of a brain contained within it.

A more precise 3D computational model can be synthesized from the set of magnetic resonance imaging (MRI) images which retain high-quality details of the organ tissues. The MRI images are available on a medical data site [3]. The target organ is scanned to generate 53 consecutive images, each image consisting of three image components: the Proton Density Image, the T1-weighted image, and the T2-weighted image. The combination of the grayscale images of three layers forms seven distinct elements as parts of an actual human head. In

Manuscript received on February 28, 2022; revised on April 23, 2022; accepted on June 9, 2022. This paper was recommended by Associate Editor Piya Kovintavewat.

[1]The authors are with the Department of Electrical Engineering, Kasetsart University, Bangkok, Thailand.

[2]The author is with the College of Computing, Prince of Songkla University, Phuket Campus, Phuket, Thailand.

[†]Corresponding author: fengtpj@ku.ac.th

Digital Object Identifier: 10.37936/ecti-eec.2022203.247522

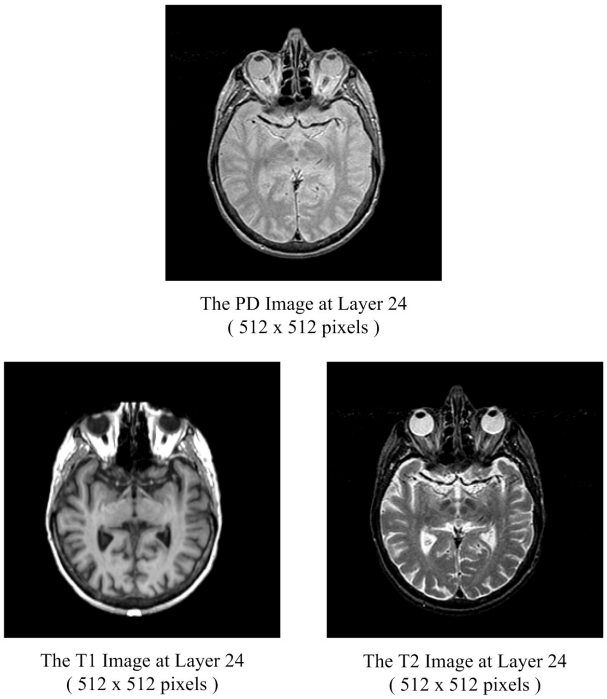

***Fig. 1**: A sample of the PD, T1, and T2 images.*

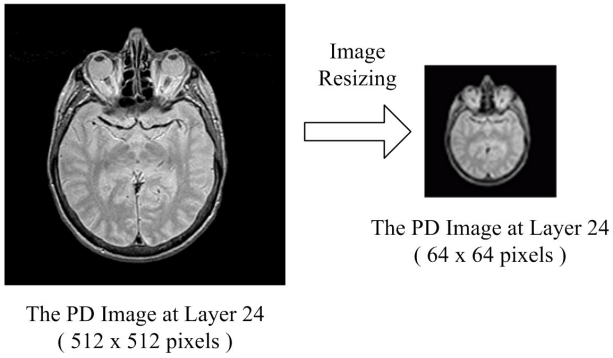

***Fig. 2**: Image resizing process.*

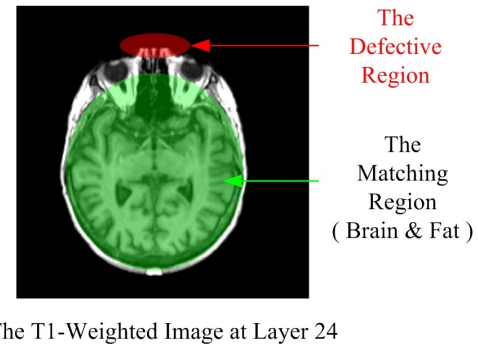

***Fig. 3**: The defective region.*

[4], the baseline detail of the electromagnetic interaction with a human head is illustrated using a finite-different time-domain (FDTD) simulation. It indicates that the elements are identified as skin, bone, muscle, fat, brain, eye, and blood. Furthermore, the information on where those elements are located is already implied by the series of images. Each element comes with its own frequency-dependent electromagnetic (EM) properties, such as dielectric constants, permittivity, and conductivity. The values of the EM properties are available on the website of the Foundation for Research on Information Technologies in Society USA, Inc. (IT'IS Foundation) [5]. It should be noted that the density of all tissues is expressed in units of kg/m^3, which is a common SI standard.

The SAR simulation is based on an FDTD method in which the head model is formed by a uniform cubical cell known as Yee's cell. Meanwhile, the mobile handset is represented by a dipole antenna. The absorbing boundary is assumed to be a perfect match, allowing for a reduction in computational burden. Other factors involved in the EMR simulation are the simulation time stepping and the weight and size of the human head. The major outputs of the simulation are the SAR and the absorbed power.

2. CREATION OF THE HUMAN HEAD MODEL

Fig. 1 shows typical MRI images for a layer of the human head cross-section: the proton density (PD) image, T1-weighted image (T1 image), and T2-weighted image (T2 image). The PD image indicates the type of tissue based on the density of the pixel dots and thus the locations of the skin, bone, and muscle in the head. The T1 image indicates the location of the brain and fat, while the T2 image depicts the blood and eyes. These can then be used to create an appropriate model for the practical simulation of EMR.

2.1 MRI Image Resizing

The original MRI images consist of 512 × 512 pixels, which is too large for the EM radiation simulation. When a 3D model is created, the total number of cells in the physical domain becomes relatively huge. Therefore, the first step is to resize the original MRI images into a 64 × 64 pixel image, as shown in Fig. 2. For a 53-layer series of MRI images, a total of 159 images will be used to create the 3D head model.

2.2 Tissue Synthesis for the Human Head Model

The findings reveal that on some T1 MRI images, areas may not be perfectly formed. An example of such an imperfect image is shown in Fig. 3. Nevertheless, it is still sufficiently informative to construct the human head module. The detail of the locations in the brain and fat are still present.

The tissues on the resized MRI images can be identified by the 8-bit grayscale intensity. The types of tissue versus the ranges of the 0–255 gray level values are listed in Table 1 [4].

It should be noted that values from 0 to 59 reflect the empty air space in the head, particularly the cavities in

***Table 1**: Tissue identification by grayscale [4].*

Gray Level	Tissue
0–59	Air
60–89	Skin
90–109	Bone
110–129	Muscle
130–159	Fat
160–199	Brain
200–219	Eye
220–255	Blood

***Table 2**: Dielectric material properties at 2.6 GHz [5].*

Tissue Type	Relative Permittivity (ε_r)	Conductivity (σ, S/m)	Density (ρ, kg/m^3)
Air	1	0	1
Skin	37.8	1.54	1109
Bone	11.3	0.424	1908
Muscle	52.5	1.84	1090
Fat	10.8	0.288	911
Brain	48.7	1.91	1045
Eye	51.064	2.086	1053
Blood	58	2.68	1050

the nose and ears. The EM properties of air are, of course, the base of other materials. Taking this into account in the head model is expected to deliver more accurate results.

2.3 Material Properties of Head Tissues

Once the tissue types are identified, the next step to creating the head model is to assign the tissue with the relevant EM properties. Two key material properties are the relative permittivity (ε_r) and conductivity (σ), both of which are frequency-dependent. A collection of the EM properties is listed in Table 2 [5]. Note that although air is not a tissue, it can be located in the human head, and its properties do not vary with frequency.

The dielectric parameters are simplified to some extent as the tissue properties are not homogenous and also condition-dependent. Since the nature of the tissue may vary in detail and composition some assumptions are necessary for the simulation.

i) The tissue type is judged by the majority of tissues within the cell of interest. It is considered to be a homogenous tissue.
ii) The values of the dielectric parameters are averaged from that of the composite tissues. For example, a pair of eyes takes an average parameter of the composite tissues of the aqueous humor, choroid, ciliary body, cornea, iris, lens, retina, sclera, vitreous humor, cortex, and nucleus. Meanwhile, the brain takes an average parameter from the composite tissues of the neurons, dendrites, axons, glial cells, and capillaries.

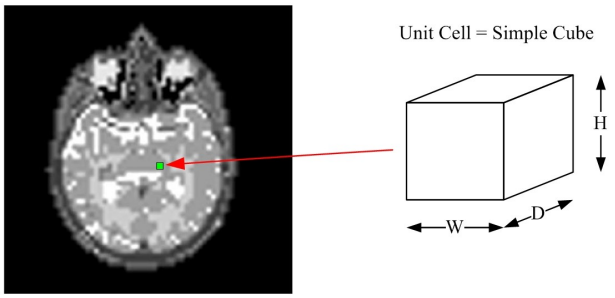

***Fig. 4**: Sample of a unit cell.*

iii) The tissue conditions are taken from the most typical. For example, dry skin and a cortical-type bone.
iv) The values of the dielectric parameters are calculated according to the frequency of tissue occurrence.

2.4 Unit Cell of the Human Head Model

In this work, the 3D unit cell is represented by a cube with an identical width W, depth D, and height H. The volume is, thus, simply given as:

$$V = W^3 \tag{1}$$

The size comparison and the head model are illustrated in Fig. 4. The unit cell is assumed to be homogenous, i.e., the cell contains only one tissue. Consequently, a specific set of particular dielectric parameters can be assigned for the unit cell.

3. SIMULATION DOMAIN

In this simulation, the computational domain can be separated into two parts: the physical region (domain) and the artificial absorbing environment (domain). The physical region consists of the human head, mobile handset, and air space. The first two interact with each other through an air gap in the middle. In the simulation, the air space or air gap is basically the free-space medium whose permittivity (ε_0) and permeability (μ_0) are 8.854×10^{-12} F/m and $4\pi \times 10^{-7}$ H/m, respectively. The artificial absorbing environment is assumed to be the perfectly matched layer (PML), where neither additional radiation nor reflection occurs.

Fig. 5 shows the configuration of the simulation domain. The cellular handset device radiates a power of 0.6 W. The handset is placed away from the head for a distance of $\Delta\ell$, which can accommodate two unit cells. In this case, the EM interaction dominates the unit cells that are simply like a propagation along a distance $\Delta\ell$.

3.1 Simulation Based on Maxwell's Equations

The EM simulation is performed using a collection of Maxwell's equations to solve the values. In this work, Maxwell's equations, based on the newly generalized perfectly matched layer [6], are applied to simulate the behavior of the EM propagation on the computer. The equations are valid for both the physical and artificial

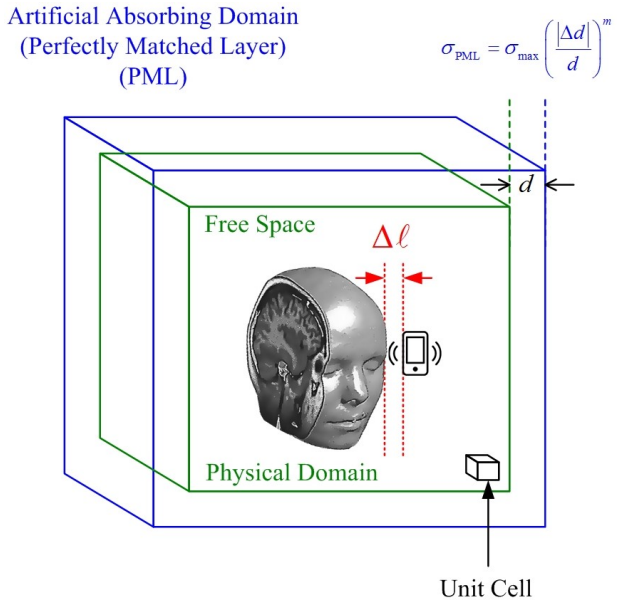

***Fig. 5**: Simulation domain.*

absorbing domains. The commonly used formulas can be expressed as:

$$\nabla \times \vec{H} = j\omega\varepsilon_0\hat{\varepsilon}_r(\omega)\overline{\varepsilon}\vec{E} \tag{2}$$

$$\nabla \times \vec{E} = -j\omega\mu_0\hat{\mu}_r(\omega)\overline{\mu}\vec{H} \tag{3}$$

It should be noted that Eqs. (2) and (3) are actually the same and subsequently brought into the finite different time-domain (FDTD) method.

One important parameter in the equations is the relative permittivity $\varepsilon_r(\omega)$. This frequency-dependent permittivity is described as:

$$\hat{\varepsilon}_r(\omega) = \varepsilon_r(\omega) + \frac{\sigma(\Omega)}{j\omega\varepsilon_0}, \quad \hat{\mu}_r(\omega) = 1 \tag{4}$$

The terms $\overline{\varepsilon}$ and $\overline{\mu}$ are expressed by:

$$\overline{\varepsilon} = \overline{\mu} = \begin{bmatrix} \frac{a_y a_z}{a_x} & 0 & 0 \\ 0 & \frac{a_x a_z}{a_y} & 0 \\ 0 & 0 & \frac{a_x a_y}{a_z} \end{bmatrix} \tag{5}$$

where $a_i = 1 + \left(\sigma_i / j\omega\varepsilon_0\right)$. For the perfectly matched layer, the conductivity in this domain is given by Eq. (6).

In addition, it clearly refers to the conductivity of the perfectly matched layer which lies between the boundaries of the free space (Δd) and distance (d):

$$\sigma_{\text{PML}} = \sigma_{\max}\left(\frac{|\Delta d|}{d}\right)^m \tag{6}$$

The value is proportional to the m^{th} power of the ratio of the free space(Δd) and the PML distance (d).

The simulation time step (Δt) follows the principles of the Courant-Friedrichs-Lewy stability criterion (CFL) [7]:

$$\Delta t < \left(c\sqrt{\frac{1}{\Delta x^2} + \frac{1}{\Delta y^2} + \frac{1}{\Delta z^2}}\right)^{-1} \tag{7}$$

where $c = 3 \times 10^8$ m/s.

As can be observed, the parameter Δt is a constraint when choosing the aforementioned unit cell size. For a unit cell size of 5.0 × 5.0 × 5.0 mm^3, the required time step Δt becomes 9.62×10^{-12} s [8]. A finer cell size leads to a smaller time step and hence, more computational load.

3.2 Specific Absorption Rate (SAR)

The investigation of the specific absorption rate (SAR) is based on the following relationship:

$$\text{SAR 1g} = \sigma\frac{|E|^2}{\rho} \tag{8}$$

According to the standard of the Federal Communications Commission (FCC) [9], the value of the SAR 1g is limited to 1.6 W/kg when measured on a weight of 1 g. In previous investigative work on SAR [8], 1 g of the weight is approximately covered by seven unit cells (0.970375 g). One of the challenges in this work is that the size of the unit cell needs to be adjusted so that 1 g is accurately covered by an integer number of the unit cells.

3.3 Absorbed Power

The absorbed power is another measure in the investigation of radiation and is defined as the amount of radiation energy trapped in the human head. The instantaneous power is determined by the sum of the instantaneous electric field intensity squared over a certain volume, expressed as:

$$P(t) = \int_V \sigma |E(t)|^2 dV \tag{9}$$

According to the previous work [8], the absorbed power at 2.6 GHz resulting from a handset with an output power of 0.6 W placed at a distance of 1 cm from the head is 0.06939 W (11.56579%).

4. RESULTS

This section contains the key results of the research for the results head model and the responses of both the SAR and absorbed power.

4.1 Head Model with the Size of Unit Cells

Fig. 6 presents a graphical cross-sectional view of the MRI images used to construct the human head model. Since the original high-resolution images of 512 × 512 pixels are resized to 64 × 64 pixel images, the total cells formed by 53 layers equates to 217 088 cells. Each cell is then classified into one of the tissues listed in Table 2. The numbers of tissue cells are summarized in Table 3. It should be noted that these include the air cells surrounding the head. In the simulation domain, the

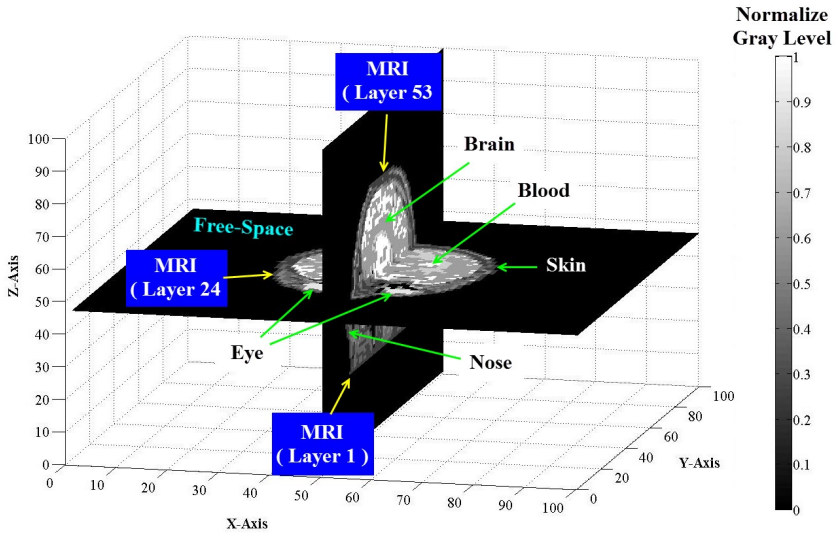

***Fig. 6**: Software used for human head modeling.*

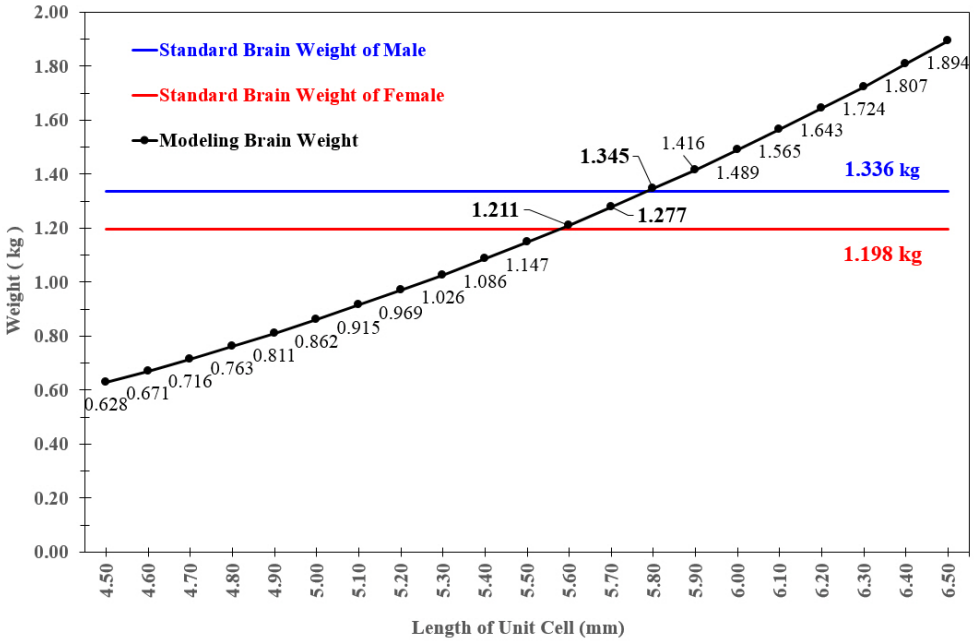

***Fig. 7**: Modeling brain weight.*

total number of tissue cells in the head is 74 685, which is just 34.40% or approximately one-third of the total cells created from the MRI images.

Due to variations in the actual size of the head and gender differences, one pixel on the MRI image cannot convert directly to the physical size of the unit cell. This work offers a solution to this problem by invoking the constraint on brain weight. This reverse engineering approach is deployed.

The total number of brain cells of 6598 either represents the average female brain weight of 1.198 kg or a male brain weight of 1.336 kg [10]. In both cases, the tissue density is 1045 kg/m^3. The calculated brain weights, starting with a cell width of 4.5 to 6.5 mm, are summarized with the percentage deviations from the average values presented in Table 4 and Fig. 7. According to the calculation, the cell sizes with low errors for both genders are found in the range of 5.6 to 5.8 mm. The 5.6 mm cell size is the best fit for females, while the 5.8 mm cell is the best fit for males. Since the gender is not given, a female is assumed. Therefore, in this work, the size selected for the unit cell is 5.6 mm.

Fig. 8 shows the construction of a unit cell measuring 5.6 mm. The head model width and depth are 24.64 cm (44 × 0.56 cm) and 32.48 cm (58 × 0.56 cm), respectively.

4.2 EM Simulation Results at 2.6 GHz

The simulation is set as follows: a unit size of 5.6 mm is the size of choice. The parameter $\Delta\ell$ shown in Fig. 5

***Table 3**: Number of tissues in the human head model and surrounding area.*

Tissue Type	Number of Tissues	Density (kg/m^3)
Air	142 403	1
Skin	21 200	1109
Bone	14 025	1908
Muscle	8149	1090
Fat	19 302	911
Brain	6598	1045
Eye	254	1053
Blood	5157	1050

is set to 1.12 cm with a power of 0.6 W and an operating frequency of 2.6 GHz. This leads to a time step (Δt) value of 0.01 ns.

4.2.1 Penetration of 0.6 W transmit power

Fig. 9 illustrates the EM intensity caused by a mobile handset placed 1.12 cm away from the head. The left image is observed for a time duration of $500\Delta t$ (5 ns) and the right for $1000\Delta t$ (10 ns) to demonstrate how the radiation penetrates the brain.

Fig. 10 shows the EM intensity when the distance $\Delta\ell$ of the mobile handset is placed at 1.12 and 11.2 cm (10 times further). The time duration is set to 10 ns ($1000\Delta t$). As expected, the further the distance, the less EM intensity manifests in the head model. Placing the handset at 1.12 cm, the EM shows greater penetration into the brain than is the case with a distance of 11.2 cm. The absorbed power tends to be significantly more than when the mobile is placed further away from the head.

4.2.2 SAR versus head-handset separation

Fig. 11 illustrates the linear plots for SAR 1g and SAR 10g values when 0.6 W is radiated at a varying distance, $\Delta\ell$, of between 1.12 and 11.20 cm with a distance step of 1.12 cm. Five nearest unit cells and 50 unit cells are used to determine the SAR 1g and SAR 10g, respectively. The SAR value diminishes as the distance between the handset and the head increases. Compared to the FCC limit of 1.6 W/kg, all values from this setup meet the FCC standard.

4.2.3 Absorbed power versus head-handset separation

Using the same setup, Fig. 12 shows the absorbed power in watts versus the distance gap between the handset and head. With an operating frequency of 2.6 GHz, the overall absorbed power tends to decrease as the gap increases. However, it is not a monotonic decrease because, at some distances, specifically between 3 and 6 cm, the simulation results show an unusual rise in absorbed power.

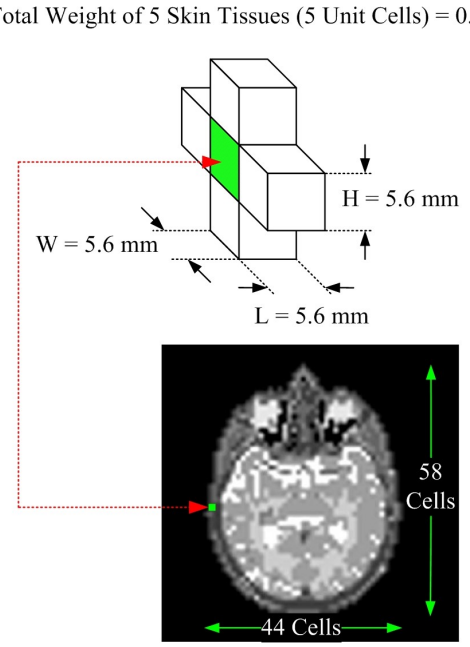

***Fig. 8**: Size of the human head model.*

4.2.4 Power levels versus FCC limit

In order to investigate whether the critical radiated power still meets the FCC standards for the SAR, the transmitted power of the handset is varied from 0.1 to 2.0 W. The separation distance $\Delta\ell$ is maintained at 1.12 cm. The EM intensity in the head model is shown in Fig. 13 for 0.1 W (left) and 1.0 W (right). The higher the power, the deeper the penetration into the head.

Fig. 14 shows SAR 1g and SAR 10g versus the transmitted power. It can be observed that the difference between SAR 1g and SAR 10g increases along with the transmitted power. The critical transmitted powers driving the SAR to the FCC limit are 0.8 and 0.9 W for SAR 1g and SAR 10g, respectively.

Fig. 15 indicates the absorbed power versus the radiated power. The absorbed power linearly increases from 7 mW to 145 mW as the radiated power is raised from 0.1 to 2.0 W.

5. CONCLUSION

The 3D human head model in this study is created using a collection of MRI images. This research work is based on two factors relating to the human head; dimensions and average brain weight. The types and locations of tissues are identified, and the frequency-dependent EM properties assigned for the 5G mid-band frequency at 2.6 GHz. With respect to the average brain weight, the optimized unit cell of $5.6 \times 5.6 \times 5.6$ mm^3 is used in the structural model of the human head. By shaping 74 685 cells, the average adult size of a virtual human head is achieved with dimensions of 24.64 cm, 32.48 cm, and 29.68 cm in width, depth, and height, respectively.

The SAR effect and absorbed powers are investigated using the resultant human head model. In the

***Table 4**: Brain weight approximation.*

Length of unit cell (m)	Brain 6598 cells 1045 kg/m^3	Percentage error (% Error), the average brain weight of an adult female = 1.198 kg	Percentage error (% Error), the average brain weight of an adult male = 1.336 kg
0.0045	0.628	−47.554	−52.972
0.0046	0.671	−43.980	−49.766
0.0047	0.716	−40.246	−46.418
0.0048	0.763	−36.350	−42.925
0.0049	0.811	−32.289	−39.283
0.0050	0.862	−28.058	−35.489
0.0051	0.915	−23.655	−31.541
0.0052	0.969	−19.075	−27.434
0.0053	1.026	−14.316	−23.167
0.0054	1.086	−9.374	−18.735
0.0055	1.147	−4.245	−14.136
0.0056	1.211	1.073	−9.367
0.0057	1.277	6.585	−4.424
0.0058	1.345	12.294	0.695
0.0059	1.416	18.203	5.993
0.0060	1.489	24.316	11.475
0.0061	1.565	30.636	17.142
0.0062	1.643	37.166	22.998
0.0063	1.724	43.911	29.046
0.0064	1.807	50.873	35.289
0.0065	1.894	58.06	41.73

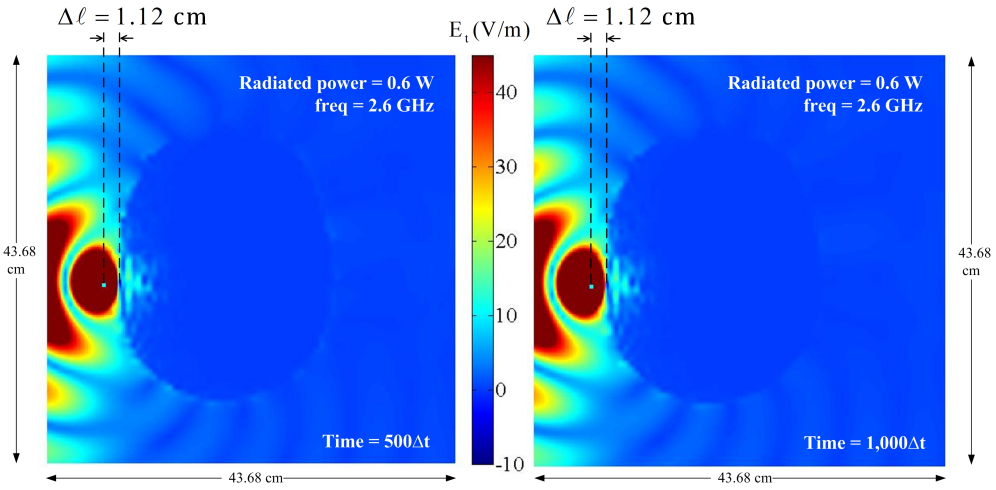

***Fig. 9**: EM intensity for $\Delta\ell$ = 1.12 cm with observation times of 500Δt (left) and 1000Δt (right).*

simulation, the unit cell size requires a time step of 0.1 ns. The numerical results illustrate the response of the SAR/absorbed power versus the transmitted power with varying distances between the handset and head. The EM intensity in the head model is provided to monitor the penetration depth. Based on a parametric study using the FDTD method, the results show that a sensitive distance below 2.0 cm results in a strong effect of the SAR 1g together with high absorbed power. When varying the radiated power, the responses of both of these are slightly linear when the power is increased. To meet the FCC margin of the SAR 1g effect at 1.6 W/kg, the transmitted power of 0.8 W is limited to achieve the maximum power for controlling the operation of a mobile handset. This indicates that the absorbed power in the human head represents 7.268% of the transmitted power from the handset.

REFERENCES

[1] B. B. Beard and W. Kainz, "Review and standardization of cell phone exposure calculations using the SAM phantom and anatomically correct head models," *BioMedical Engineering OnLine*, vol. 3, 2004, Art. no. 34.

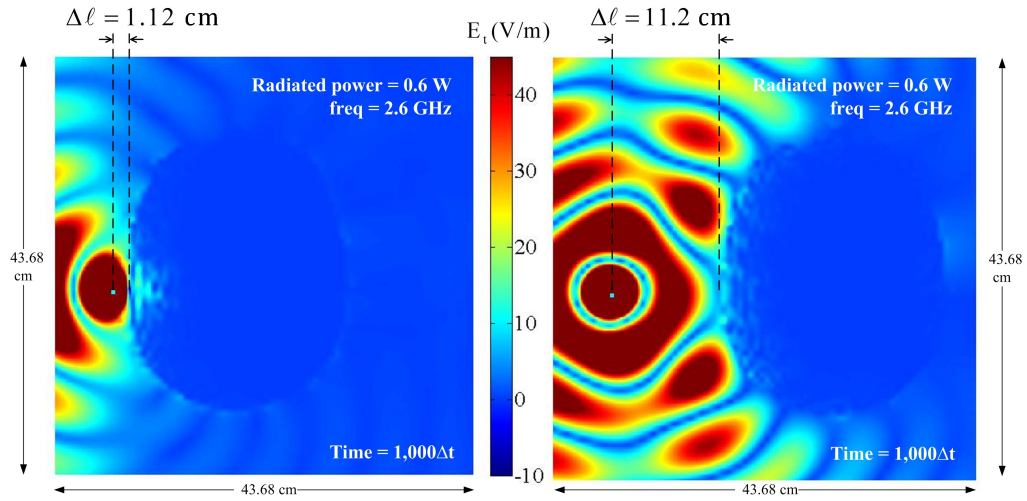

***Fig. 10**: EM intensity at a time of 1000Δt with two different mobile distances, Δℓ = 1.12 cm (left) and Δℓ = 11.2 cm (right).*

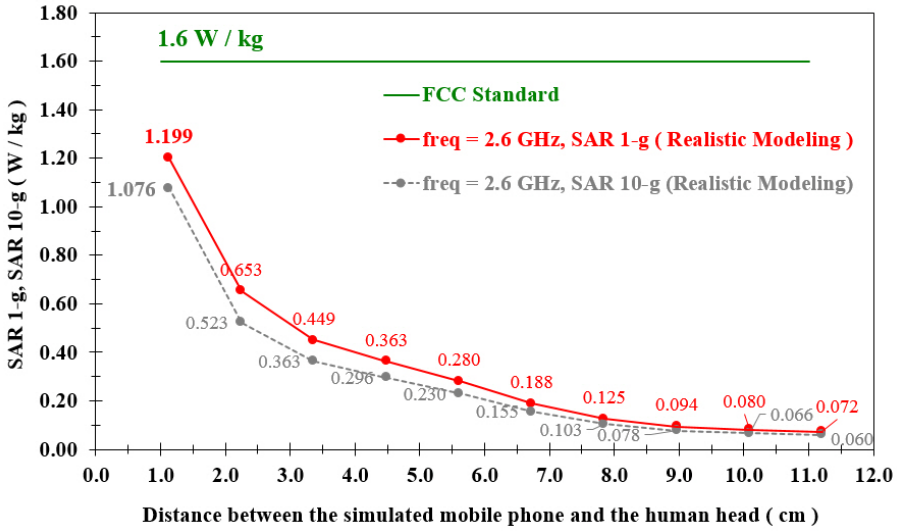

***Fig. 11**: Simulation results of the SAR 1g and SAR 10g at various distances.*

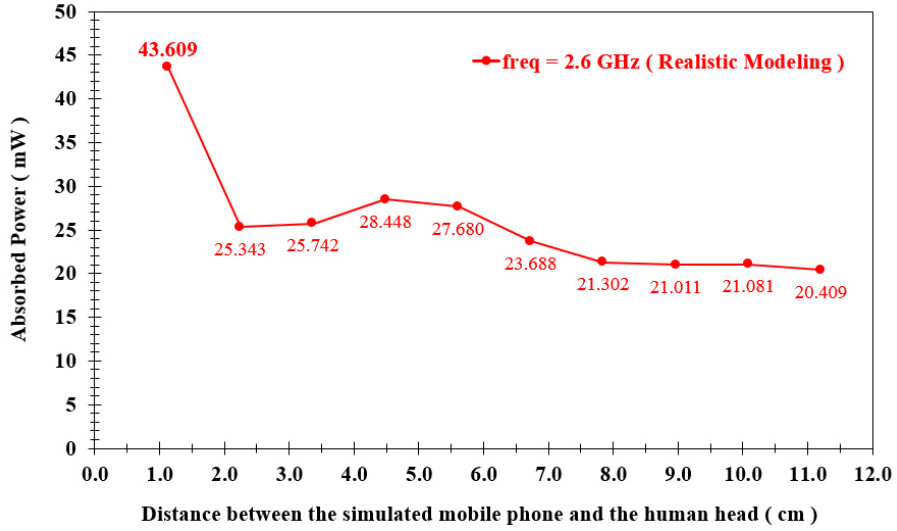

***Fig. 12**: Absorbed power within the human head model at various distances.*

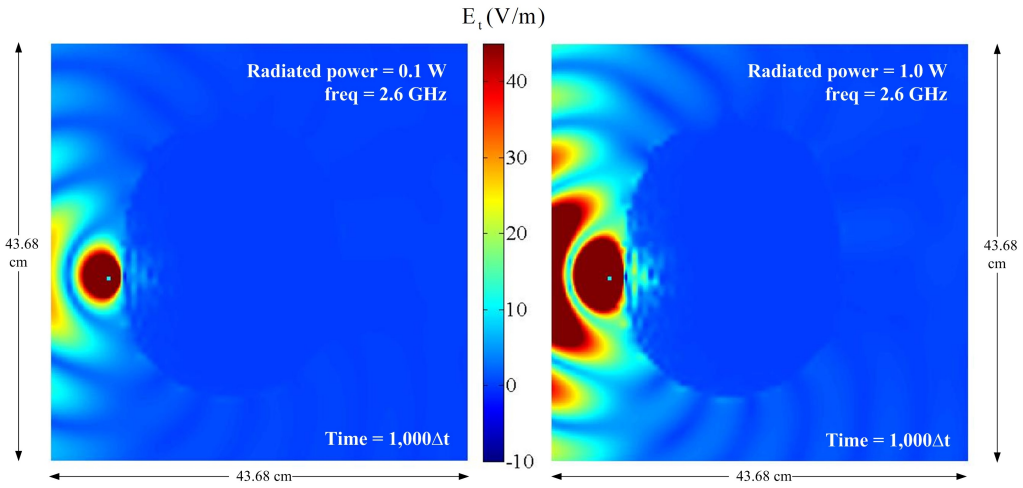

***Fig. 13**: Radiated Power = 0.1 W (left) and 1.0 W (right) at 1000Δt.*

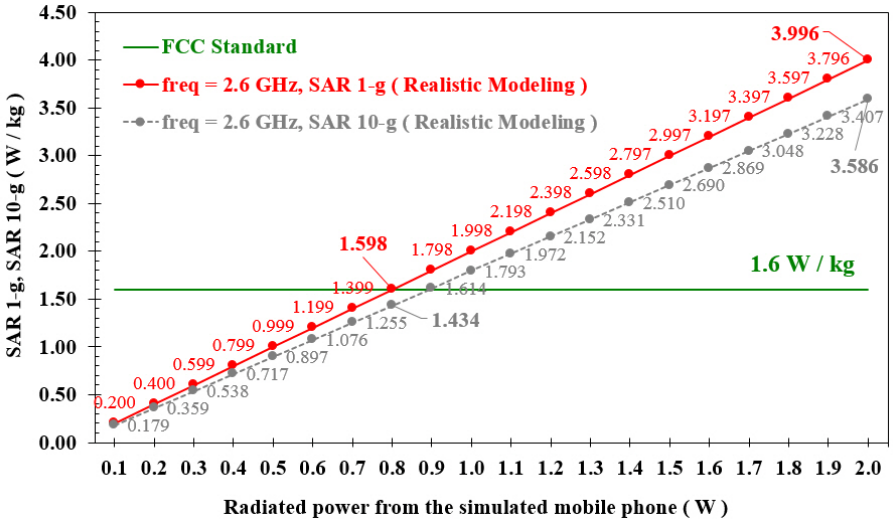

***Fig. 14**: Comparison of SAR 1g, SAR 10g, and FCC limit for various radiated powers.*

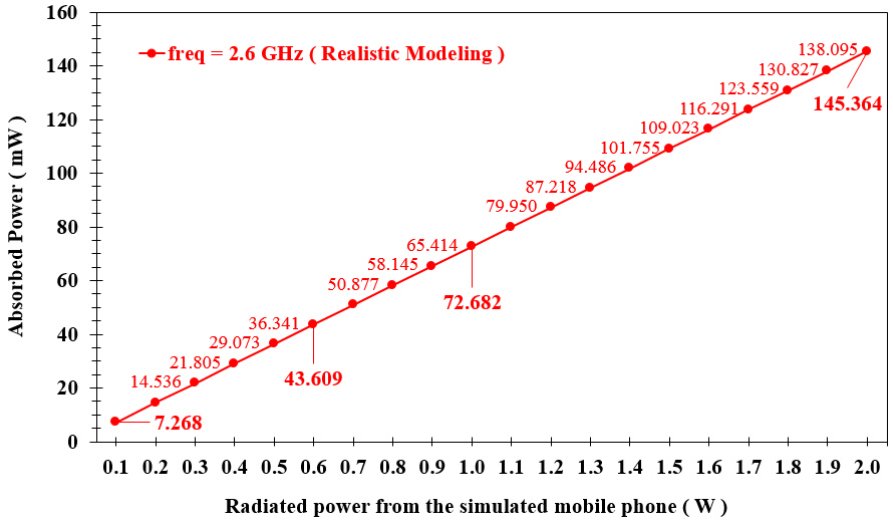

***Fig. 15**: Absorbed power in the human head model radiated power from 0.1 to 2.0 W.*

[2] A.-K. Lee, S.-E. Hong, J.-H. Kwon, and H.-D. Choi, "SAR comparison of SAM phantom and anatomical head models for a typical bar-type phone model," *IEEE Transactions on Electromagnetic Compatibility*, vol. 57, no. 5, pp. 1281–1284, Oct. 2015.

[3] K. A. Johnson and J. A. Becker. The whole brain atlas. https://www.med.harvard.edu/aanlib/ (accessed Oct. 10, 2021).

[4] A. Z. Elsherbeni, C. D. Taylor, and Y. R. Samii. Real time simulation of the interaction of electromagnetic waves with a human head. http://home.olemiss.edu/~atef/head/headpresentation/index.html (accessed Oct. 13, 2021).

[5] IT'IS Foundation. Dielectric properties. https://itis.swiss/virtual-population/tissue-properties/database/dielectric-properties/ (accessed Oct. 10, 2021).

[6] L. Ling, L. Ronglin, X. Suming, and N. Guangzheng, "A new generalized perfectly matched layer for terminating 3d lossy media," *IEEE Transactions on Magnetics*, vol. 38, no. 2, pp. 713–716, Mar. 2002.

[7] C. Gabriel, "Compilation of the dielectric properties of body tissues at RF and microwave frequencies," Armstrong Laboratory (AFMC), Occupational and Environmental Health Directorate, Radiofrequency Radiation Division, Brooks Air Force Base, Texas, USA, Tech. Rep. AL/OE-TR-1996-0004, Jan. 1996.

[8] T. Jariyanorawiss and W. Chongburee, "A report on human head exposure to a 2.6 GHz mid-band of 5G by using FDTD method," in *2020 17th International Conference on Electrical Engineering/Electronics, Computer, Telecommunications and Information Technology (ECTI-CON)*, 2020, pp. 808–811.

[9] Specific absorption rate (SAR) for cellular telephones. https://www.fcc.gov/general/specific-absorption-rate-sar-cellular-telephones (accessed Jan. 30, 2022).

[10] P. Hartmann, A. Ramseier, F. Gudat, M. J. Mihatsch, W. Polasek, and C. Geisenhoff, "Normal weight of the brain in adults in relation to age, sex, body height and weight," (in German), *Der Pathologe*, vol. 15, no. 3, pp. 165–170, Jun. 1994.

Terapass Jariyanorawiss received his B.Eng., M.Eng. and D.Eng. degree in Electrical Engineering from Kasetsart University, Bangkok, Thailand. His research interests include computational electromagnetic, computer network, IoT and blockchain.

Komsan Kanjanasit received his B.Eng. degree from Rajamangala Institute of Technology, Patumthanee, Thailand, the M.Eng. degree from King Mongkut's Institute of Technology North Bangkok, Bangkok, Thailand, and the Ph.D. degree from Heriot-Watt University, Edinburgh, UK, all in electrical engineering, in 2001, 2005, and 2015, respectively. He is currently an assistant professor with the College of Computing, Prince of Songkla University, Phuket Campus, Thailand. His research interests include antennas, metamaterials, microfabrication, sensors and intelligent objects.

Wachira Chongburee received his Ph.D. in Electrical Engineering from Virginia Tech, USA in 2003. He has joined Kasetsart University, Thailand as a faculty member for 20 years. He severed the Office of National Telecommunication Commission as a radio equipment standard committee member. He is also now serving Council of Engineers, Thailand on EE curriculum certifying for the practical engineering licensing.